HNUE JOURNAL OF SCIENCE
Natural Sciences 2025, Volume 70, Issue 4, pp. 88-100
This paper is available online at http://hnuejs.edu.vn/ns
DOI: 10.18173/2354-1059.2025-0057

MORPHOLOGICAL AND PHASE EVOLUTION OF COBALT SULFIDE ON CARBON CLOTH VIA CONTROLLED HYDROTHERMAL SYNTHESIS FOR HIGH-PERFORMANCE FLEXIBLE SUPERCAPACITORS

Nguyen Dinh Hung[1] Dang Van Cu[2], Le Quang Huy[1],
Luong Thi Thu Thuy[1] and Le Van Khu[1,*]
[1]*Faculty of Chemistry, Hanoi National University of Education, Hanoi city, Vietnam*
[2]*Vietnam - Korea Institute of Science and Technology, Hanoi city, Vietnam*
*Corresponding author: Le Van Khu, email: khulv@hnue.edu.vn

Received December 1, 2025. Revised December 20, 2025. Accepted December 30, 2025.

Abstract. Cobalt sulfide nanoparticles were successfully synthesized on carbon cloth (CC) via a one-step hydrothermal method, with varying precursor ratios, hydrothermal temperatures, and hydrothermal times. The crystalline structure, morphology, and composition of the as-prepared CoS were analyzed using X-ray diffraction (XRD), Raman spectroscopy, scanning electron microscopy (SEM, and energy-dispersive X-ray spectroscopy (EDS). Structural analyses confirmed the formation of the hexagonal phase of CoS. Electrochemical measurements revealed that the CoS electrode, prepared with a Co:S ratio of 1:2 at 160 ^{o}C for 15 h, exhibited the highest specific capacitance of 424 F g^{-1} at a current density of 1 A g^{-1} and 350 F g^{-1} at a current density of 5 A g^{-1}. Moreover, the electrode also demonstrated excellent cycling stability, retaining approximately 90 % of its initial specific capacitance after 1000 charge-discharge cycles at a current density of 2 A g^{-1}. These results highlight a facile, cost-effective, easy-to-implement, and efficient method for utilizing cobalt sulfide-based electrodes for flexible supercapacitor applications.

Keywords: cobalt sulfide, carbon cloth, flexible supercapacitor.

1. Introduction

As modern society progresses rapidly, the demand for compact, lightweight, intelligent, and wearable devices for medical, military, and civilian use applications has increased significantly. Consequently, flexible energy storage devices have therefore become a research area of interest to many scientists [1]. In this regard, the flexible capacitor stands out as more appealing compared to lithium-ion batteries, thanks to their naturally high power density, rapid charge/discharge performance, extended lifespan,

and mechanical adaptability. However, most commercially available supercapacitors are still based on rigid materials. Therefore, developing stretchable and flexible electrode materials to replace conventional rigid electrodes is expected to be a key direction in the future advancement of supercapacitor technologies.

For supercapacitors, achieving high energy capacity and power capability is a crucial requirement. Among the promising materials, cobalt sulfide pseudocapacitive compounds stand out due to their high theoretical capacitance (almost 3000 F g^{-1} [2]), which arises from the reversible surface redox reactions. Additionally, cobalt sulfide is low-cost, earth-abundant, and environmentally benign, so it was widely explored for various energy-related applications. However, the synthesis of electrodes is typically fabricated by mixing active materials with binders and conductive materials and pressing them onto a flexible surface, resulting in poor and unstable adhesion that affects the electrochemical performance of supercapacitors when subjected to mechanical stresses, such as folding or twisting.

Furthermore, the binder is electrochemically inactive, limiting the energy/power density of the electrode [3]. Therefore, synthesizing high-purity cobalt sulfide directly onto flexible substrates without the use of templates or binders remains a significant challenge. This difficulty arises because cobalt sulfide exists in a wide range of chemical compositions, increasing the possibility of forming complex phases. Furthermore, cobalt ions exhibit a strong affinity for oxygen, which complicates the removal of cobalt oxide or hydroxide impurities during synthesis [4]. For example, during the synthesis of cobalt sulfide, Alshoaibi A. reported the formation of a CoO co-product [5], Acharya D *et al.* observed dual-phase cobalt sulfide/cobalt oxyhydroxide [6], and Kumar N *et al.* obtained CoS_2 and Co_9S_8 [7]. Among the methods of synthesizing materials for flexible capacitors, namely, electrochemical, one-step or two-step hydrothermal calcine [8], solvothermal [9], etching and sulfurization [10], oxidation and sulfuration [11], and printing, etc., hydrothermal is a simple, easy to apply, and offers effective control over the material structure and morphology by adjusting the synthesis conditions [12].

Herein, we demonstrate the fabrication of a binder-free flexible electrode with excellent electrochemical properties via a single hydrothermal process. Conductive carbon cloth (CC) was used as both a flexible current collector and a substrate for the in- situ growth of cobalt sulfide as an active material for supercapacitors. The effects of synthesis conditions, including precursor ratio, hydrothermal temperature, and hydrothermal time, on the structure and morphology of the as-prepared materials as well as their electrochemical properties, were investigated. Results show the applicability of cobalt sulfide materials for flexible supercapacitors.

2. Content

2.1. Experiment

2.1.1. Hydrothermal synthesis of cobalt sulfide on carbon cloth

Carbon cloth (10 mm × 30 mm) was cleaned by soaking in acetone and ethanol under sonication to remove the surface organic compound before drying at 60 - 70 °C. The washed carbon cloth was wrapped with Teflon tape to define a 1 cm^2 active area.

Cobalt sulfide was synthesized hydrothermally using ethanol solutions of $Co(NO_3)_2 \cdot 6H_2O$ (0.2 M) and thiourea (0.4 M) [5]. Specified volumes of the two precursors were mixed and diluted to 25 mL, and the carbon cloth pieces were immersed in the solution inside a Teflon-lined autoclave. The autoclave was heated at the selected temperature for the prescribed time, followed by natural cooling. The electrodes were washed with hot, double-distilled water and ethanol, dried, and stored under inert conditions.

Three synthesis parameters were varied systematically: precursor molar ratio (Co: thiourea = 1:1, 1:2, 1:3, and 1:4), reaction time (9, 12, 15, 18 h), and reaction temperature (140, 150, 160, and 170 °C). All samples are denoted as CSa-x-y, where a is the precursor molar ratio (thiourea: Co), x is the hydrothermal temperature (°C), and y is the reaction time (h).

2.1.2. Characterization

The morphology and microstructure of the prepared samples were examined by Field emission scanning electron microscopy (Hitachi S-4800). Elemental composition was analyzed by Thermal field emission scanning electron microscopy **(**JSM-IT800) equipped with EDS analysis (Ultim Max 65). Crystalline phases were identified via X-ray diffraction using Bruker D8 Advance, with Cu Kα radiation (λ = 1.5406 Å), operated at 40 kV and 30 mA. The average crystallite size is calculated from XRD patterns using Scherrer's equation [5] as follows:

$$D = k\lambda/(\beta cos\theta) \quad (1)$$

where D is the crystallite size; λ is the wavelength of the X-ray source; θ is Bragg's diffraction angle in degrees, k is a constant equal to 0.9, and β is the full width at half maxima in radians. Raman spectra were recorded on LabRAM HR Evolution using a 532 nm excitation laser set at 3 mW to minimize heating effects.

2.1.3. Electrochemical measurements

Electrochemical performance was evaluated in a standard three-electrode configuration, using the cobalt sulfide growth on carbon cloth as the working electrode, a Pt foil as the counter electrode, and a Hg/HgO (1 M KOH) electrode as the reference. All measurements were carried out in a 3.0 M KOH aqueous electrolyte at room temperature using a VSP Potentiostat (BioLogic). Cyclic voltammetry (CV) and galvanostatic charge-discharge (GCD) were performed to assess the capacitive behavior. The specific capacitance C (F g^{-1}) is calculated from GCD measurement using the equation [13].

$$C = \frac{I \times \Delta t}{m \times \Delta V} \quad (2)$$

where I is the discharge current (A), Δt is the discharge time (s), m is the mass of the electroactive material (g), and ΔV is the potential window (V).

2.2. Results and discussion

2.2.1. Characterizations

**** Morphological evolution of cobalt sulfide nanostructure on carbon cloth***

The cobalt sulfide nanostructures evolved systematically with varying hydrothermal conditions, showing a transition from sheet-like to nanoparticle morphologies. At lower temperatures, such as CS2-140-15 (140 - 150 °C) (Figure 1a & 1b) or short reaction time (≤ 12 h) (Figure 1c & 1d), the products consisted of thin, loosely connected nanosheets, reflecting incomplete nucleation and limited crystal growth. Increasing the temperature and time promoted the conversion to discrete nanoparticles through thermally activated nucleation and recrystallization [14].

Varying the precursor ratio also influenced structural evolution: sulfur-deficient conditions Co:S = 1:1) yielded small, compact particles (Figure 1e), whereas sulfur excess (Co:S ≥ 1:3) produced irregular nanosheets and dense aggregates (Figure 1f & 1g). Under optimized conditions of 160 °C for 15 h at a Co:S ratio of 1:2 (Figure 1h), uniform quasi-spherical nanoparticles with diameters of 50 - 70 nm densely covered the carbon cloth, indicating balanced nucleation and growth kinetics. Further increasing the temperature to 170 °C (Figure 1i) or prolonging the reaction to 18 h (Figure 1k) led to a coalesced cluster due to Ostwald ripening and thermal sintering.

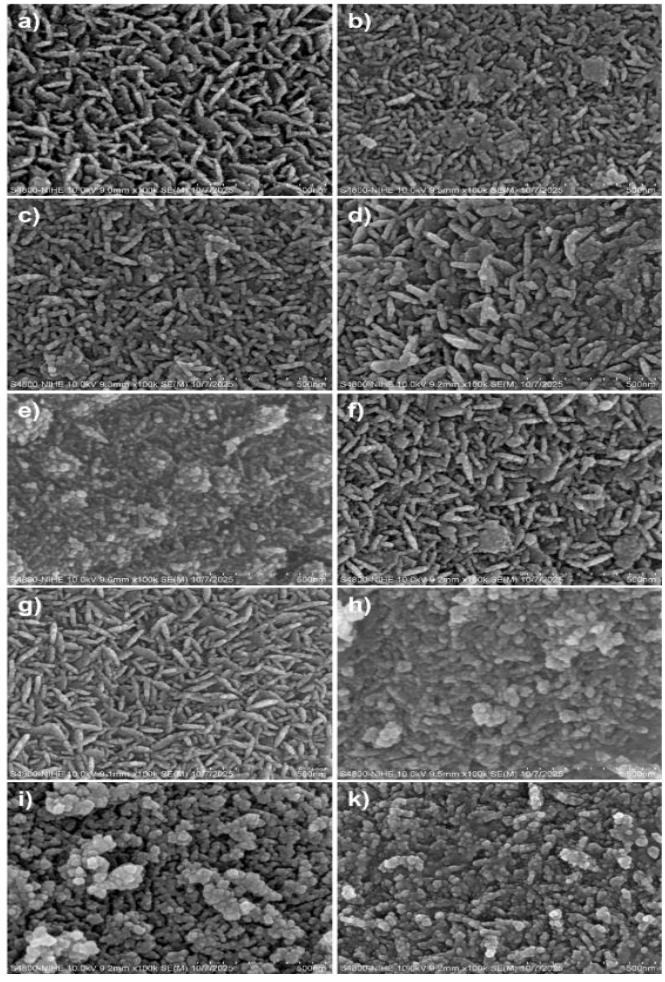

Figure 1. SEM images of cobalt sulfide growth on carbon cloth were synthesized at different hydrothermal conditions

**** Compositional and stoichiometric analysis***

EDX spectra revealed the coexistence of Co, S, O, and C in the samples (Figure 2). The detected carbon and oxygen signals primarily originated from the substrate and surface oxidation, respectively. Quantitative EDX analysis (Table 1) revealed that atomic ratios of the samples synthesized at Co/S = 1:1, 1:2, 1:3, and 1:4 were 1.81, 1.96, 1.34, and 1.41, respectively. This trend demonstrates that cobalt-rich compositions predominate across all samples, whereas increasing sulfur precursor concentration results in only a moderate enhancement of sulfur incorporation. Notably, the CS2-160-15 sample exhibited the lowest oxygen content (6.6 wt %), indicating minimal oxidation and high sulfide phase purity. These compositional results align with the morphological observations, supporting that the Co:S ratio of 1:2 promotes balanced nucleation and efficient sulfidation.

Table 1. EDX analysis of synthesized cobalt sulfide at different precursor ratios

Samples	Molar ratio of Co/S	Weight percentage (wt.%)			
		Co	*S*	*O*	*Total*
CoS1-160-15	1.81:1	70.00±3.33	21.00±1.29	9.00±2.28	100
CoS2-160-15	1.96:1	72.13±1.55	21.27±0.97	6.60±0.74	100
CoS3-160-15	1.34:1	63.07±2.89	25.62±0.79	11.31±2.18	100
CoS4-160-15	1.41:1	66.12±1.62	25.58±1.01	8.30±0.64	100

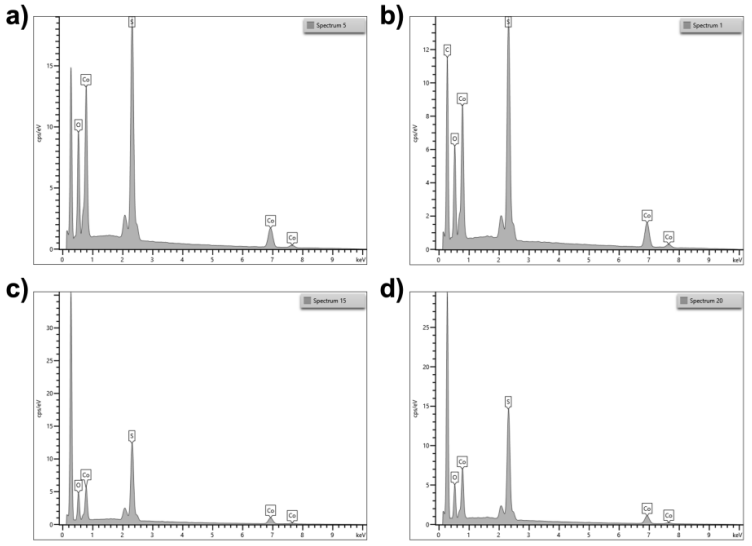

Figure 2. EDX spectra of (a) CS1-160-15, (b) CS2-160-15, (c) CS3-160-160-15, and (m) CS4-160-15

**** Phase identification and structural evolution (XRD analysis)***

X-ray diffraction patterns (Figure 3) demonstrated that all synthesized samples contain crystalline cobalt sulfide phases. The diffraction peaks located at 2θ = 30.9°, 35.6°, 47.1, and 54.9° correspond to the (100), (101), (102), and (110) planes of

hexagonal CoS (PDF #65-3418). The sharpness and intensity of these peaks varied markedly with synthesis conditions, reflecting the degree of crystallinity and phase purity.

When the reaction time increased from 9 to 15 h at 160 °C (CS2-160-9 → CS2-160-15), the diffraction peaks intensified and narrowed, indicating enhanced crystallinity and enlarged crystalline size (Figure 3a). However, a weak additional peak at 2θ = 55.2°, which is attributed to the (311) plane of cubic CoS_2 (PDF #65-3322), was detected in CS2-160-9 and CS2-160-18, suggesting that incomplete or prolonged reactions may promote the coexistence of sulfur-rich phases. At 15 h (CS2-160-15), this CoS_2 disappeared, confirming complete conversion to the stable CoS phase. Therefore, 15 h is identified as the optimal duration yielding phase-pure CoS with high crystallinity.

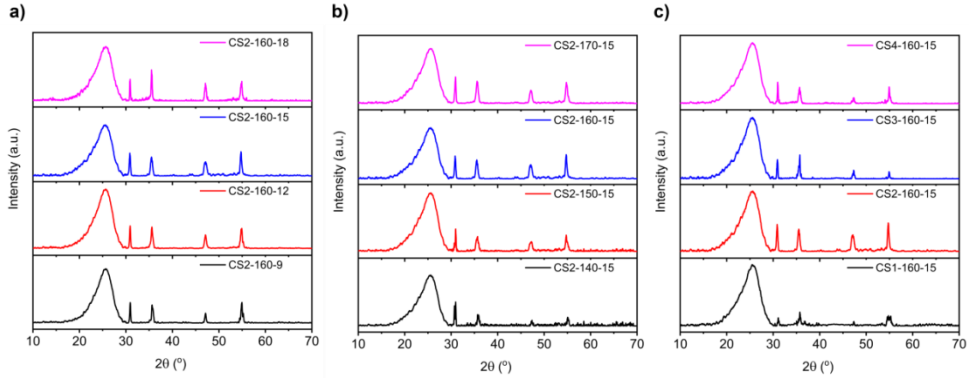

Figure 3. XRD patterns of cobalt sulfide growth on carbon cloth synthesized under different hydrothermal conditions: (a) time, (b) temperature, and (c) precursor ratio

At 140 °C (CS2-140-15 in Figure 3b), peak splitting and broadening were observed for the (100), (101), and (102) reflections, revealing structural disorder and lattice distortion due to insufficient crystal growth. Increasing the temperature to 160 °C eliminated peak splitting and enhanced overall intensity, reflecting complete phase conversion and relaxation of crystal defects. At 170 °C (CS2-170-15), peak intensity plateaued, indicating that further temperature increases did not significantly improve crystallinity but could induce partial sintering.

Varying the precursor ratio also influenced phase formation (Figure 3c). The CS1-160-15 sample, synthesized at a ratio Co:S = 1:1, showed weak and broad peaks, indicative of poor crystallinity. As the sulfur ratio increased to 1:2 in CS2-160-15, the diffraction peaks became sharper and more intense, confirming enhanced crystallite growth and phase purity with an average crystallite size of 19.12 nm. Ratios above 1:2 resulted in broader peaks again, suggesting over-sulfidation and possible defect formation. Therefore, a Co:S = 1:2, 160 °C temperature, and 15 h duration were identified as optimal for producing well-crystallized, single-phase CoS nanostructures.

**** Raman spectroscopy analysis***

Raman spectra further confirmed the formation and structural integrity of cobalt sulfide. Apart from the characteristic D and G bands of carbon cloth at ~1340 and 1590 cm^{-1} [15], all samples exhibited distinct vibrational modes associated with CoS. The peaks at 260, 463, 505, and 660 cm^{-1} correspond to Co-S bending (E_g), Co-S stretching (F_{2g}), and S-S stretching (A_{1g}) modes of CoS, respectively (Figure 4) [16], [17].

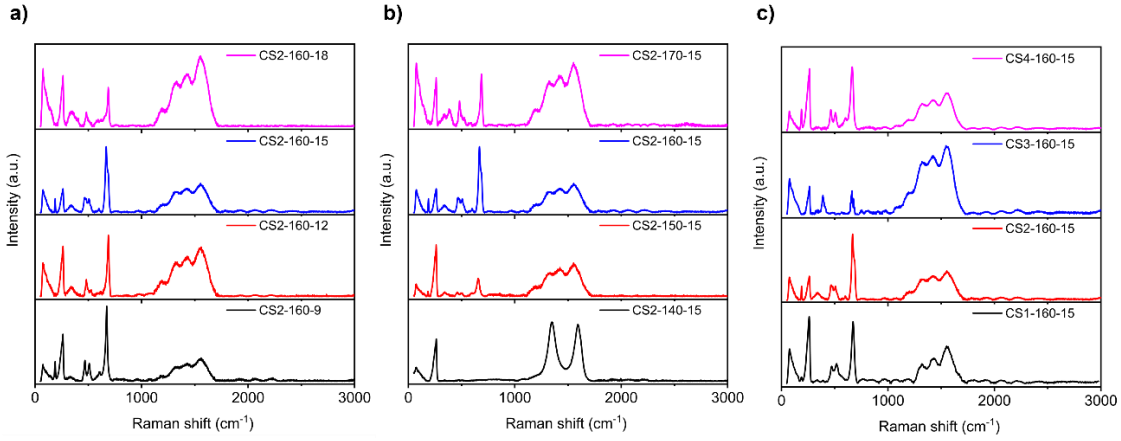

Figure 4. Raman spectra of cobalt sulfide growth on carbon cloth synthesized under different hydrothermal conditions: (a) time, (b) temperature, and (c) precursor ratio

As the reaction time and temperature increased, these Raman peaks became sharper and more intense, reflecting improved crystalline ordering and reduced defect density (Figure 4a & 4b). In contrast, the samples prepared for 9 and 12 h (CS2-160-9 and CS2-160-12) showed broader peaks with weak intensity, suggesting incomplete crystallization. In addition, CS2-160-18 displayed a reduced A_{1g} peak at 660 cm^{-1}, implying partial reformation of CoS_2 species, consistent with the XRD results. Similarly, the sample synthesized at 160 °C for 15 h with Co:S = 1:2 showed the most pronounced Raman features, confirming that this condition produced the most ordered CoS phase.

**** Correlation between structure and formation mechanism***

The combined SEM, EDX, XRD, and Raman results reveal a consistent formation pathway of cobalt sulfide nanostructures on carbon cloth under hydrothermal conditions (Scheme 1). The evolution of morphology and crystallinity is determined by the interplay of precursor chemistry, temperature, and reaction time.

Initially, Co^{2+} ions form coordination complexes with thiourea molecules. Upon heating, thiourea decomposes to release H_2S and CN_2H_2, providing S^{2-} ions that react with Co^{2+} to nucleate cobalt sulfide species on the carbon cloth surface. As the reaction proceeds, the nuclei grow through diffusion and Ostwald ripening into uniform CoS nanoparticles. The optimized parameters (160 °C, 15 h, and Co:S = 1:2) enable balanced nucleation and growth, yielding phase-pure CoS with high crystallinity and intimate contact with the carbon substrate.

When the reaction is prolonged or sulfur concentration is excessive, partial resulfurization and aggregation occur, resulting in CoS_2 impurity formation and reduced uniformity. This mechanistic correlation explains the observed transition from sheet-like to spherical morphologies and from disordered to well-crystallized CoS structures as the synthesis parameters are optimized.

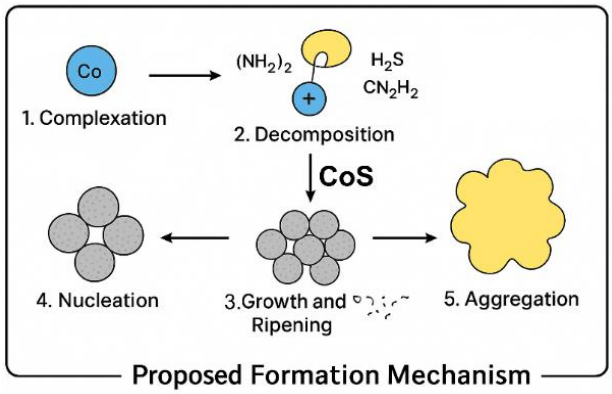

Scheme 1. Proposed formation mechanism of cobalt sulfide

2.2.2. Electrochemical performance

The electrochemical properties of the cobalt sulfide electrodes grown on carbon cloth were systematically evaluated in a three-electrode system using 3.0 M KOH as electrolyte. The measurements, including cyclic voltammetry (CV) and galvanostatic charge-discharge (GCD), were performed to elucidate the charge-storage behavior and the influence of the synthesis parameter on the capacitive performance.

**** Redox behavior and charge-storage mechanism***

Figure 5a shows representative CV curves of the optimized CoS electrode (CS2-160-15) at different scan rates. Two distinct redox couples located at approximately 0.18/0.14 V and 0.52/0.50 V (*vs.* Hg/HgO) are observed, corresponding to the sequential oxidation of $Co^{2+} \rightarrow Co^{3+}$, and $Co^{3+} \rightarrow Co^{4+}$ during the faradaic process [18]. These reactions can be expressed as [8]:

$$CoS + OH^- \rightleftharpoons CoSOH + e^- \quad (3)$$

$$CoSOH + OH^- \rightleftharpoons CoSO + H_2O + e^- \quad (4)$$

The presence of well-defined redox peaks and a quasi-rectangular shape indicates that both faradaic and double-layer capacitance contribute to the total charge storage. The area enclosed by the CV curves increases proportionally with the scan rate, suggesting fast and reversible redox kinetics facilitated by the intimate contact between CoS nanostructures and the conductive carbon substrate.

Figure 5b compares the GDC profiles of the CoS electrode synthesized at different temperatures and reaction times at a current density of 1 A g^{-1}. All electrodes exhibit non-linear charge-discharge curves with evident voltage plateaus, which deviate from the ideal triangular shape of electric double-layer capacitors. This behavior confirms that the charge storage process is dominated by reversible faradaic reactions associated with $Co^{2+}/Co^{3+}/Co^{4+}$ redox couples, in good agreement with the CV results discussed above. In addition, the GDC curves of CS2-160-15 electrode recorded at different current densities ranging from 1 to 5 A g^{-1} (Figure 5c) indicate its excellent rate capability and highly reversible redox reactions. The superior performance of CS2-160-15 can likely be attributed to the optimized crystallinity of the material at the synthesized conditions [5], as confirmed by the XRD analysis.

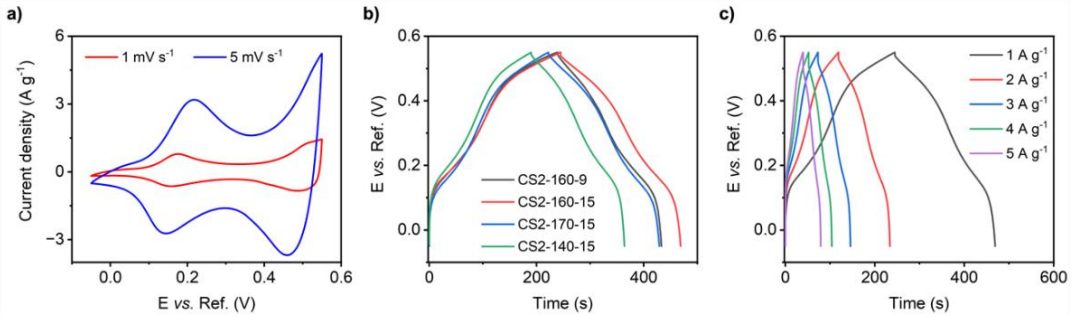

Figure 5. (a) CV curves of CS2-160-15, (b) GDC profiles at 1 A g^{-1} of several CoS electrodes, and (c) GDC profiles of CS2-160-15 at various current densities

**** Effect of the synthetic parameter on capacitive behavior***

The specific capacitance of the cobalt sulfide electrodes shown in Figure 6, as calculated from GCD measurements at current densities ranging from 1 to 5 A g^{-1}, shows a clear dependence on hydrothermal temperature, reaction duration, and precursor composition. In general, increasing the synthesis temperature from 140 to 160 °C (CS2-140-15 → CS2-160-15) markedly enhances the specific capacitance from 307 to 424 F g^{-1} at 1 A g^{-1}, whereas a further increase to 170 °C decreases the specific capacitance to 367 F g^{-1} (Figure 6a). This evolution indicates that moderate temperatures promote the formation of a highly porous and electrochemically active nanostructure, while excessive heating induces particle coarsening and structural densification, thereby reducing accessible area. Despite the lower absolute capacitance, the 170 °C sample (CS2-170-15) exhibits the highest rate capability, maintaining 89.4% of its initial value at 5 A g^{-1}, which suggests improved electrical connectivity and shortened ion-transport paths in the more compact structure. Reaction time also exerts a non-linear influence on the capacitive response. When the temperature is fixed at 160 °C, extending the hydrothermal duration from 9 h to 15 h (CS2-160-9 → CS2-160-15) increases the specific capacitance from 364 to 424 F g^{-1}, followed by a slight drop to 367 F g^{-1} at 18 h (Figure 6b). The improvement up to 15 h can be attributed to sufficient nucleation and growth of cobalt sulfide nanostructures that yield a larger electroactive surface and optimized porosity. Over-prolonged treatment, however, promotes crystallite agglomeration and reduced ion accessibility, leading to diminished performance with the lowest specific capacitance of 298 F g^{-1} at 5 A g^{-1} for CS2-160-18.

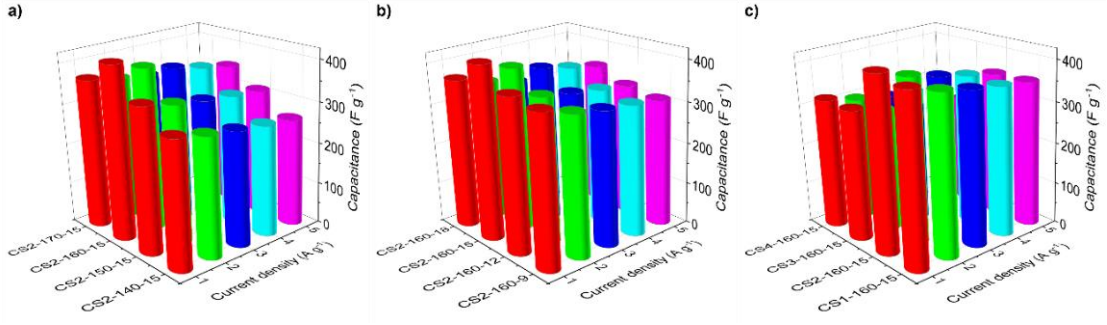

Figure 6. Capacitance of cobalt sulfide growth on carbon cloth synthesized under different hydrothermal conditions: (a) temperature, (b) time, and (c) precursor ratio

The precursor ratio further modulates the capacitive behavior by tuning the Co:S stoichiometry (Figure 6c). Among the four compositions (CS1 → CS4) prepared at 160 °C for 15 h, the CS1- and CS2-based electrodes deliver the highest specific capacitance of 411 and 424 F g^{-1}, respectively, whereas CS3- and CS4-based electrodes exhibit lower values (318 F g^{-1}). The EDX analysis of the Co/S ratio in the prepared materials indicates that samples CS1- and CS2- exhibit values of 1.81:1 and 1.96:1, while samples CS3- and CS4- only achieved ratios of 1.34:1 and 1.41:1. The reduction in capacitive performance at low sulfur precursor ratios suggests that this parameter indirectly influences the electric and ionic pathways for charge storage through its impact on stoichiometric sulfur in the as-prepared electrodes. Among all tested conditions, the CS2-160-15 sample demonstrates the best overall electrochemical performance, achieving a high specific capacitance of 424 F g^{-1} at 1 A g^{-1} and retaining 82.5% (350 F g^{-1}) at 5 A g^{-1}. The capacitance of the CS2-160-15 electrode is comparable or even superior to that of CoS on flexible substrates (285.8 F g^{-1} at 2 A g^{-1} [8]), or on rigid substrates (420 F g^{-1} at 1 A g^{-1} for $Co_{1-x}S$ on nickel foam [19], 357 F g^{-1} at 0.5 A g^{-1} of flower-like CoS on nickel foam [20]).

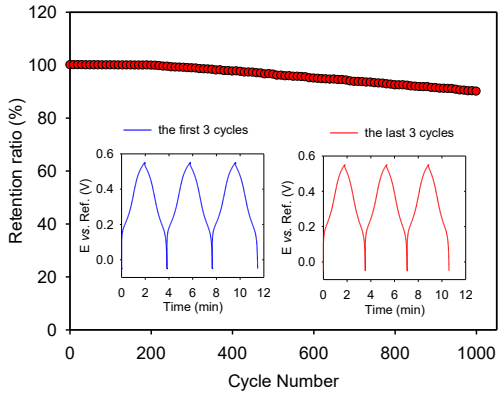

Figure 7. Capacitance retention as a function of number of charge–discharge cycles at 2 A g^{-1} (inset figure shows the first and the last three cycles of charge–discharge curves)

Cycling measurements were conducted at a current density of 2 A g^{-1}. The result demonstrates stable electrochemical behavior up to 1000 charge-discharge cycles, with the retention of 90% of its initial capacity (Figure 7).

**** In-depth analysis and mechanistic interpretation***

The CS2-160-15 electrode represents the optimal equilibrium between kinetics and thermodynamics during hydrothermal synthesis. Its superior capacitance (424 F g^{-1} at 1 A g^{-1}) arises from a well-crystallized CoS framework with abundant redox-active sites and efficient ion diffusion channels. To elucidate the charge storage mechanism of CS2-160-15, the dependence of specific capacitance on the scan rate was analyzed using the Trasatti method, which deconvolutes the total capacitance into outer-surface (electrochemically accessible at all scan rates) and diffusion-controlled (scan rate dependent) contributions. According to this approach, the specific obtained from CV measurements (Figure 8a) follows two characteristic relationships: 1/C varies linearly with $\nu^{0,5}$, and C varies

linearly with $\nu^{-0,5}$. These correlations arise from the fact that at high scan rates only the outer surface of the electrode is accessible for charge storage, whereas at low scan rates ions have sufficient time to penetrate the inner active sites governed by semi-infinite diffusion.

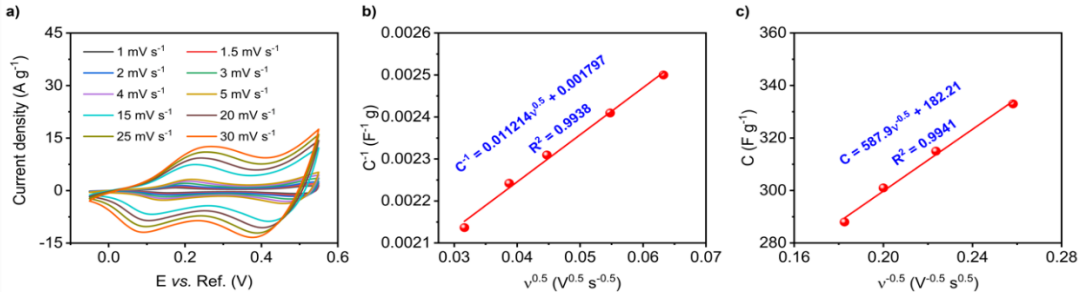

Figure 8. (a) CV curves at various scan rates, plots of (b) C^{-1} vs. $\nu^{0.5}$, and (c) C vs. $\nu^{-0.5}$

Extrapolation of 1/C *vs.* $\nu^{0.5}$ plot to $\nu = 0$ yields the total capacitance (outer-surface plus diffusion-controlled) (Figure 8b), while the intercept of C *vs.* $\nu^{-0.5}$ plot at infinite scan rate ($\nu \rightarrow \infty$) (Figure 8c) represents the purely surface-controlled capacitance. The difference between these two values quantitatively corresponds to the diffusion-controlled contribution. Therefore, linearity in both plots with high R^2 validates the applicability of the Trasatti model and confirms that a combination of surface pseudocapacitance and diffusion-limited processes governs the measured capacitive response.

The quantitative analysis shows that only ~33% of the total capacitance originates from fast surface reactions, while the bulk diffusion process contributes the majority (~67%), confirming a hybrid charge-storage mechanism. Rate capability analysis reveals CV retention ≈61.5% at a scan rate of 30 mV s^{-1} and GCD retention ≈82.5% at a current density of 5 A g^{-1}. Although the CS2-170-15 synthesized at a higher temperature (170 °C) exhibits slightly better rate retention (~70%), its lower total capacitance confirms that enhanced surface contributions alone cannot compensate for reduced bulk activity. Hence, CS2-160-15 achieves the most balanced configuration between surface pseudocapacitance and bulk redox storage. The temperature-time correlation further supports this interpretation. Increasing reaction time or temperature enhances crystallization and electron transport up to an optimal point (15 h, 160 °C), beyond which overgrowth and sulfur excess hinder diffusion and interfacial charge transfer. Therefore, the optimized synthesis condition reflects a delicate balance between redox kinetics and phase stability.

3. Conclusions

The cobalt sulfide/carbon cloth was synthesized via hydrothermal reaction under varying conditions. At a Co:S ratio of 1:2, a hydrothermal temperature of 160 °C, and a duration of 15 h, the resulting material exhibited well-crystallized, single-phase hexagonal CoS with hemispherical nanoparticles measuring 50-70 nm in diameter. Electrochemical characterization in a 3 M KOH electrolyte revealed pseudocapacitive behavior with Co^{2+}/Co^{3+} and Co^{3+}/Co^{4+} redox peaks in cyclic voltammetry. The CS2-160-15 exhibited a maximum specific capacitance of 424 F g^{-1} at a current density

of 1 A g^{-1}. At higher scan rates, charge storage was predominantly limited to the electrode outer surface, whereas at lower scan rates, ions were able to diffuse and access inner active sites and were governed by a semi-infinite diffusion process. Furthermore, the electrode exhibited remarkable cycling stability, retaining 90% of its initial specific capacitance even after 1000 charge-discharge cycles. Experiment results highlighted the influence of hydrothermal synthesis conditions on the capacitive performance of the CoS/CC electrode and underscore its potential for applications in flexible energy storage devices.

Acknowledgments. This work was supported by the Vietnamese Ministry of Education and Training under Grant No. B2024-SPH-09.

REFERENCES

[1] Yan Z, Luo S, Li Q, Wu ZS & Liu S, (2023). Recent advances in flexible wearable supercapacitors: Properties, fabrication, and applications. *Advanced Science*, 11, 2302172.

[2] Halder A, Aman M, Lichchhavi & Jha SK, (2024). Enhancing supercapacitor performance with binder-free cobalt sulfide pseudo-capacitive electrodes: A path to sustainable energy storage. *Journal of Electroanalytical Chemistry*, 972, 118631.

[3] Rathinamala I, Manohara Babu I, Johnson William J, Muralidharan G & Prithivikumaran N, (2021). Extra-durable hybrid supercapacitor based on cobalt sulfide and carbon (MWCNT) matrix electrodes. *Journal of Energy Storage*, 34, 102200.

[4] Sayah A, Bahloul A, Habelhames F, Boumaza N, Ghalmi Y, Tounsi A, Lamiri L, Nessark B, Ghelani L, Chala A, (2025). Electrodeposition mode effects on the electrochemical performance of cobalt sulfide material for supercapacitors. *Ionics*, 31, 851-864.

[5] Alshoaibi A, (2023). Investigating the supercapacitive performance of cobalt sulfide nanostructures prepared using a hydrothermal method. *Materials*, 16, 4512.

[6] Acharya D, Ko TH, Bhattarai RM, Muthurasu A, Kim T, Saidin S, Choi JS, Chhetri K & Kim HY, (2023). Double-phase engineering of cobalt sulfide/oxyhydroxide on metal-organic frameworks derived iron carbide-integrated porous carbon nannofibers for asymmetric supercapacitors. *Advanced Composites and Hybrid Materials*, 6, 179.

[7] Kumar N, Raman N & Sundaresan A, (2014). Synthesis and properties of cobalt sulfide phases: CoS_2 and Co_9S_8. *Zeitschrift für anorganische und allgemeine Chemie*, 60, 1069-1074.

[8] Miya LA, Ghosh SK, Kumari P, Mbileni Morema CN & Mallick K, (2025). Eco-friendly and sustainable supercapacitor design: Cobalt sulfide nanoparticles embedded on carbon cloth as an electrode material for asymmetric devices. *Chemical Paper*, 79, 7617-7631.

[9] Wang YX, Tsai DS, Huang CJ, Chen ZY & Lee CP, (2025). One-step synthesis of Zirconium sulfide nanoparticles on flexible carbon cloth for supercapacitor application. *Batteries*, 11, 138.

[10] Yin S, Kong L, Du Y, Wei W & Shen X, (2024). $Co_{1-x}S$/N, S-codoped carbon loaded porous carbon cloth as a flexible electrode for high-performance supercapacitors. *Chemical Engineering Journal*, 499, 156517.

[11] Cui M, Park SJ & Kim S, (2024). Flexible N-doped heterostructure of cobalt sulfide and cobalt oxide composite electrodes derived from metal-organic frameworks and their electrochemical behaviors. *Inorganic Chemistry Communications*, 159, 111805.

[12] Xiong X, Waller G, Ding D, Chen D, Rainwater B, Zhao B, Wang Z & Liu M, (2015). Controlled synthesis of $NiCo_2S_4$ nanostructured arrays on carbon fiber paper for high-performance pseudocapacitors. *Nano Energy*, 16, 71-80.

[13] Zhu J, Xiang L, Xi D, Zhou Y & Yang J, (2018). One-step hydrothermal synthesis of flower-like CoS hierarchitectures for application in supercapacitors. *Bulletin of Materials Science*, 41, 54.

[14] Wan H, Ji Xiao, Jiang J, Yu J, Miao L, Zhang Li, Bie S, Chen H & Ruan Y, (2013). Hydrothermal synthesis of cobalt sulfide nanotubes: The size control and its application in supercapacitors. *Journal of Power Sources*, 243, 396-402.

[15] Zhao W, Chao L, Gaofeng S, Guoying W, Qi Z, Hongquan Z, Ying S, Jianglei Y, Xin, Fenfang L, Yawen H & Kaiquiang Y, (2020). Electrospinning CoS_2/carbon nanofibers with enhanced stability as electrode materials for supercapacitors. *Ionics*, 26, 5737-5746.

[16] Dui M, Bo H, Wenda W, Xi L, Jiantao, Chen S, Tsegaye Tadesse T, Liwei C, Xuefeng Q & Leo L, (2019). Highly active nanostructured CoS_2/CoS heterojunction electrocatalysts for aqueous polysulfide/iodide redox flow batteries. *Nature Communications*, 10, 3367.

[17] Kangle L, Aixiang W, Weiwei Z, Zhiming X, Yu Z & Jun L, (2018). Synthesis of vertically aligned CoS prismatic nanorods as counter electrodes for dye-sensitized solar cells. *Journal of Materials Science: Materials Electron*, 40, 1541-1546.

[18] Wang Q, Jiao L, Du H, Yang J, Huan Q, Peng W, Si Y, Wang Y & Yuan H, (2011). Facile synthesis and superior supercapacitor performances of three-dimensional cobalt sulfide hierarchitectures. *CrystEngComm*, 13, 6960-6963.

[19] Ranaveera C, Wang Z, Alqurashi E, Kahol PK, Dvornic P, Gupta BK, Ramasamy K, Mohite AD, Gupta G & Gupta RK, (2016). Highly stable hollow bifunctional cobalt sulfides for flexible supercapacitor and hydrogen evolution. *Journal of Materials Chemistry A*, 23, 9014-9018.

[20] Zhu J, Xiang L, Xi D, Zhou Y & Yang J, (2018). One-step hydrothermal synthesis of flower-like CoS hierarchitectures for application in supercapacitors. *Bulletin of Materials Science*, 41, 54.